

# Printing Gel-like Catalysts for the Directed Growth of Multiwall Carbon Nanotubes

Hannes Kind,<sup>†</sup> Jean-Marc Bonard,\* László Forró, and Klaus Kern<sup>‡</sup>

*Département de Physique, École Polytechnique Fédérale de Lausanne,  
CH-1015 Lausanne EPFL, Switzerland*

Klara Hernadi

*Applied Chemistry and Environment Department, József Attila University,  
H-6720 Szeged, Hungary*

Lars-Ola Nilsson and Louis Schlapbach

*Physics Department, University of Fribourg, Pérolles, CH-1700 Fribourg, Switzerland*

*Received February 9, 2000. In Final Form: May 26, 2000*

Microcontact printing is used to transfer an Fe(III)-containing gel-like catalyst precursor from a hydrophilized elastomeric stamp to a substrate. The catalytic pattern activates the growth of multiwall carbon nanotubes using chemical vapor deposition of acetylene. Our results show that the choice of the catalyst is of extreme importance. Most of the aqueous and ethanolic Fe(III) inks used give rise to drying effects on the stamp surface, which lead to the formation of islands of the catalyst within the pattern. To avoid these shortcomings, we developed a catalyst precursor, which has better performance on the stamp and as a catalyst on the substrate. Simple aging of the ethanolic Fe(III) ink results in a polymerized gel-like catalyst, which can be printed homogeneously on the substrate with excellent contrast. Changing the concentration of the catalyst in the ink allows the density of the carbon nanotubes in the film to be tuned. A scanning anode field emission microscope was used to investigate the microscopic field emission properties of the samples. The emission images reproduce the topographical contrast nicely and prove the high quality of the patterning process.

## 1. Introduction

The central problem in successfully patterning substrates by the direct growth of carbon nanotubes<sup>1,2</sup> using chemical vapor deposition (CVD) of hydrocarbons over catalysts<sup>3–5</sup> is the choice of an appropriate combination of the substrate, the catalyst, and the way to apply the catalyst to the substrate.

First, the support material for the catalyst was found to play a key role in the type of nanotubes produced (for example, the number of walls, the diameter, and the degree of graphitization).<sup>6,7</sup> For high-quality patterning, the substrate itself must be completely passive for any decomposition of the hydrocarbon gas to occur. The surface morphology and chemistry of the substrate can then positively or negatively interact with the applied catalyst and in turn influence the growth of carbon nanotubes. Fan et al., for example, used porous silicon to interact strongly with the catalyst particles and to increase the growth rate compared to plain silicon.<sup>8</sup>

The second issue relates to the fact that the catalyst allows excellent control over the purity, quality, and dimensions of the nanotubes but also over the density, morphology, and orientation of the carbon nanotubes in the deposit. Basically, catalysts can be brought to the substrate by transport through the vapor phase (for example, by evaporation or sputtering), by impregnation with catalyst solutions, or by mechanical transfer. Depending on the method used, the chemical composition and morphology of the catalyst can be changed, which results in different types of nanotubes and their orientation on the substrate.<sup>8–16</sup> If necessary, additional treatment such as calcination, annealing, or reduction can be used to improve the selectivity of the catalyst prior to deposition.

Third, the choice of the technique to pattern the substrate with the catalyst is important because not all techniques are compatible with all substrates and catalysts. Dai and co-workers used electron-beam lithography

\* Corresponding author. E-mail: jean-marc.bonard@epfl.ch.

<sup>†</sup> Now at IBM Research, Zurich Research Laboratory, CH-8803 Rüschlikon, Switzerland.

<sup>‡</sup> Also at Max-Planck-Institut für Festkörperforschung, Heisenbergstrasse 1, D-70569 Stuttgart, Germany.

(1) Iijima, S. *Nature* **1991**, *354*, 56.

(2) Ebbesen, T. W. *Carbon Nanotubes: Preparation and Properties*; CRC Press: Boca Raton, FL, 1997.

(3) Ivanov, V.; Nagy, J. B.; Lambin, Ph.; Lucas, A.; Zhang, X. B.; Zhang, X. F.; Bernaerts, D.; Van Tendeloo, G.; Amelinckx, S.; Van Landuyt, J. *Chem. Phys. Lett.* **1994**, *223*, 329.

(4) Endo, M.; Takeuchi, K.; Kobori, K.; Takahashi, K.; Kroto, H. W.; Sakar, A. *Carbon* **1995**, *33*, 873.

(5) Hafner, J. H.; Bronikowski, M. J.; Azamian, B. R.; Nikolaev, P.; Rinzler, A. G.; Colbert, D. T.; Smith, K. A.; Smalley R. E. *Chem. Phys. Lett.* **1998**, *296*, 195.

(6) Hernadi, K.; Fonseca, A.; Piedigrosso, P.; Delvaux, M.; Nagy, J. B.; Bernaerts, D.; Riga, J. *Catal. Lett.* **1997**, *48*, 229.

(7) Kong, J.; Cassell, A. M.; Dai, H. *Chem. Phys. Lett.* **1998**, *292*, 567.

(8) Fan, S.; Chapline, M. G.; Franklin, N. R.; Tomblor, T. W.; Cassell, A. M.; Dai, H. *Science* **1999**, *283*, 512.

(9) Kong, J.; Soh, H. T.; Cassell, A. M.; Quate, C. F.; Dai, H. *Nature* **1998**, *395*, 878.

(10) Li, W. Z.; Xie, S. S.; Qian, L. X.; Chang, B. H.; Zou, B. S.; Zhou, W. Y.; Zhao, R. A.; Wang, G. *Science* **1996**, *274*, 1701.

(11) Terrones, M.; Grobert, N.; Olivares, J.; Zhang, J. P.; Terrones, H.; Kordatos, K.; Hsu, W. K.; Hare, J. P.; Townsend, P. D.; Prassides, K.; Cheetham, A. K.; Kroto, H. W.; Walton, D. R. M. *Nature* **1997**, *388*, 52.

(12) Ren, Z. F.; Huang, Z. P.; Xu, J. W.; Wang, J. H.; Bush, P.; Siegal, M. P.; Provencio, P. N. *Science* **1998**, *282*, 1105.

(13) Küttel, O. M.; Gröning, O.; Emmenegger, C.; Schlapbach, L. *Appl. Phys. Lett.* **1998**, *73*, 2113.

(14) Cassell, A. M.; Franklin, N. R.; Tomblor, T. W.; Chan, E. M.; Han, J.; Dai, H. *J. Am. Chem. Soc.* **1999**, *121*, 7975.

(15) Xu, X.; Brandes, G. R. *Appl. Phys. Lett.* **1999**, *74*, 2549.

(16) Kind, H.; Bonard, J.-M.; Emmenegger, C.; Nilsson, L.-O.; Hernadi, K.; Maillard-Schaller, E.; Schlapbach, L.; Forró, L.; Kern, K. *Adv. Mater.* **1999**, *15*, 1285.

to fabricate square holes in a poly(methyl methacrylate) (PMMA) film.<sup>9</sup> A drop of an ethanolic solution of an iron catalyst was then deposited onto the pattern and vaporized before calcination and liftoff. In a later work they showed that substrates can be patterned with Fe films by electron-beam evaporation through shadow masks.<sup>8</sup> Recently, we showed that microcontact printing ( $\mu$ CP) can be used to deposit an ethanolic solution of a catalyst for the production of films of carbon nanotubes.<sup>16</sup> A similar approach was used by Cassell et al. to print a liquid-phase catalyst precursor material to direct the growth of single-wall carbon nanotubes bridging between towers of prestructured substrates.<sup>14</sup>

Most microfabrication methods start with photolithography to form a pattern in a photoresist on the substrate. This patterned resist can then be used in one of two ways: it acts either as a protection (for example, against dry or wet etching) or as a removable mask for the deposition of material (for example, the evaporation of a metal), which is followed by a liftoff of the resist.<sup>17</sup> Although these techniques are very widely used, they are incompatible for solutions such as gels, some polymers, some organic and organometallic species, and biological molecules. To pattern these materials successfully, the patterned photoresist must be impermeable to the reagents used and the deposited material should not be compromised by the solvents used for the liftoff. Methods other than photolithography often involve a shadow mask formed from a rigid metal. The air gap between the mask and substrate makes the use of rigid shadow masks to pattern materials from solution impossible.<sup>17</sup> One micropatterning technique that circumvents some of these drawbacks is soft lithography,<sup>18–22</sup> which uses a patterned elastomer fabricated from poly(dimethylsiloxane) (PDMS) as the mask, stamp, or mold. Because the elastomer can conform to and seal reversibly against the contours of a surface, it can be used as a mask or a stamp. As PDMS is a material that is compatible with many of the liquid-phase catalyst precursors used for the production of carbon nanotubes, a better understanding of the chemistry of these precursors and their interactions with PDMS will help us develop better catalysts and procedures to pattern substrates with carbon nanotubes by soft lithography.

The current work elucidates some important aspects of using  $\mu$ CP to pattern silicon substrates with catalysts<sup>16,23–25</sup> followed by the growth of carbon nanotubes on the activated regions. In brief, a patterned and inked elastomeric stamp is used to print a catalyst as a pattern onto a substrate (Figure 1). The growth of multiwall carbon nanotubes follows from the catalytic decomposition of acetylene on the printed pattern of the catalyst. We show here the importance of the choice of catalyst to ensure the homogeneous and sufficient transfer of the catalyst precursor to the substrate. In choosing the appropriate catalyst precursor, patterns of multiwall carbon nanotubes

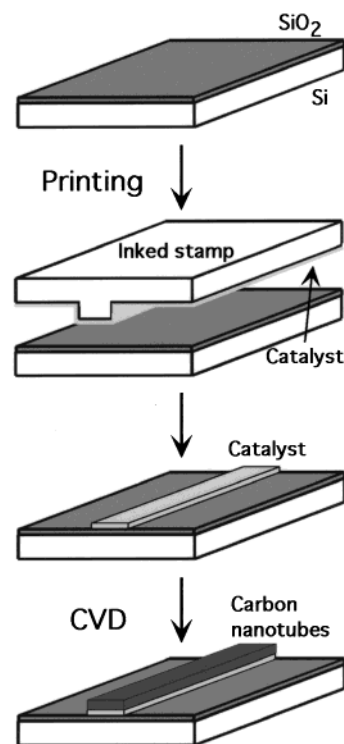


**Figure 1.** Procedure for the patterned growth of carbon nanotubes by microcontact printing a Fe(III)-based catalyst precursor onto silicon wafers. The stamp is inked with an ethanolic solution of Fe(III) and then printed onto the substrate. The growth of carbon nanotubes proceeds by the catalytic decomposition of acetylene.

can be grown with high contrast and good accuracy over large surfaces. Changing the concentration of the catalyst in the ink solution allows one to tune the density of the nanotubes from single, randomly oriented nanotubes to densely packed arrays of nanotubes oriented perpendicular to the substrate. The electron field emission properties of patterned samples are measured locally with a scanning anode field emission microscope. The emission images reproduce the grown pattern nicely and show that films of a medium density of nanotubes give rise to the highest emitter density within the features.

## 2. Experimental Section

**Materials and Substrates.** All chemicals used were of puris. p.a. quality from Fluka except for the ferric acetylacetonate (Aldrich). Absolute ethanol was used as received; water was produced with a Milli-Q Millipore purification unit. SiO<sub>2</sub>/Si wafers (Meiningen Wafer GmbH, Meiningen, Germany) were used as received. All gases had a purity of at least 99.99% (Carbagas, Lausanne, Switzerland).

Unpatterned polydimethylsiloxane (PDMS) stamps were prepared from Sylgard 184 (Dow Corning, Midland, MI) and cured for at least 12 h at 60 °C on a flat polystyrene surface (Petri dish, Falcon 1001 & 1013, Becton Dickinson Labware, NJ).<sup>26</sup> Patterned stamps were prepared similarly to flat stamps but cured on masters prepared by photolithography using Novalac resist and fluorinated with a monolayer of (1,1,2,2,-tetrahydroperfluorodecyl)trichlorosilane (ABCR, Karlsruhe, Germany). Stamps had a thickness of 4–5 mm. We used an O<sub>2</sub> plasma treatment of the stamps (oxygen pressure  $\approx$ 1 mbar, load coil power  $\approx$ 100 W, 15 s; Technics Plasma 100E, Florence, KY) to render their surface hydrophilic prior to inking. Hydrophilized stamps were stored under water before use.

(17) Madou, M. *Fundamentals of Microfabrication*; CRC Press: Boca Raton, FL, 1997.

(18) Xia, Y.; Whitesides, G. M. *Angew. Chem., Int. Ed. Engl.* **1998**, *37*, 551.

(19) Kumar, A.; Whitesides, G. M. *Appl. Phys. Lett.* **1993**, *63*, 2002.

(20) Biebuyck, H. A.; Larsen, N. B.; Delamarche, E.; Michel, B. *IBM J. Res. Dev.* **1997**, *41*, 159.

(21) Delamarche, E.; Schmid, H.; Bietsch, A.; Larsen, N. B.; Rothuizen, H.; Michel, B.; Biebuyck, H. *J. Phys. Chem. B* **1998**, *102*, 3324.

(22) Jackman, R. J.; Duffy, D. C.; Cherniavskaya, O.; Whitesides, G. M. *Langmuir* **1999**, *15*, 2973.

(23) Hidber, P. C.; Helbig, W.; Kim, E.; Whitesides, G. M. *Langmuir* **1996**, *12*, 1375.

(24) Hidber, P. C.; Nealey, P. F.; Helbig, W.; Whitesides, G. M. *Langmuir* **1996**, *12*, 5209.

(25) Kind, H.; Geissler, M.; Biebuyck, H. A.; Schmid, H.; Michel, B.; Kern, K.; Delamarche, E. *Langmuir* **2000**, *16*, 6367.

(26) Delamarche, E.; Schmid, H.; Michel, B.; Biebuyck, H. *Adv. Mater.* **1997**, *9*, 741.

**Inking and Printing.** Wet inking involved placing a drop of an aqueous or ethanolic (absolute ethanol) solution containing 10–100 mM catalyst onto a hydrophilized stamp for 15 s.  $\text{Fe}(\text{NO}_3)_3 \cdot 9\text{H}_2\text{O}$ ,  $\text{FeCl}_3$ ,  $\text{FeCl}_3 \cdot 6\text{H}_2\text{O}$ ,  $\text{Ni}(\text{NO}_3)_2 \cdot 6\text{H}_2\text{O}$ ,  $\text{Co}(\text{NO}_3)_2 \cdot 6\text{H}_2\text{O}$ , ferrocene, or ferric acetylacetonate were used as catalysts. Inks used within 2 h are referred to as fresh, whereas aged inks are those prepared more than 12 h before use. The stamp was then dried for 10 s under a continuous stream of  $\text{N}_2$ . Printing was done by placing the stamps on substrates and removing them by hand. The time of conformal contact between stamp and substrate was 3 s. For each print we used a newly patterned stamp to prevent interference from the history of the stamp with the next print. Temperature and humidity were kept constant during preparation and printing.

**Deposition of Multiwall Carbon Nanotubes.** Multiwall carbon nanotubes were deposited in a horizontal flow reactor (quartz tube of 14 mm diameter in a horizontal oven) at a reaction temperature of typically 720 °C. The samples were mounted in the tube reactor and the system was purged with 1000 mL/min of nitrogen for 15 min before a mixture of 15 mL/min of acetylene and 1000 mL/min of nitrogen was introduced at atmospheric pressure for 30 min. Finally, the system was purged again with 1000 mL/min of nitrogen for 10 min. For experiments with other pure and mixed gases ( $\text{Ar}$ ,  $\text{NH}_3$ ,  $\text{H}_2$ ) the total flows were kept constant.

**Instrumentation.** The nanotube deposits were examined using a JEOL 6300 F scanning electron microscope (SEM) operated at 5 kV. High-resolution transmission electron micrographs (TEM) were taken with a Philips CM 300 microscope operated at 300 kV. Measurements of the thickness of the printed catalyst were performed with a commercial M5 atomic force microscope (Park Scientific Instruments, Sunnyvale, CA) operated under ambient conditions in contact mode. Optical inspection of the samples and stamps was done with an Olympus BX50 microscope. UV–vis absorption spectra were obtained using a Shimadzu UV-260 spectrometer. X-ray photoemission spectroscopy (XPS) spectra were acquired on a Perkin-Elmer Phi-5500 spectrometer operating at a base pressure of  $<10^{-9}$  mbar and equipped with a monochromatized Al K $\alpha$  source ( $E = 1486.6$  eV). The analyzer was at an angle of 45° to the sample, and samples were mounted on a multisample holder stage for examination under the same conditions. Spectra are calibrated to the C 1s peak at 285 eV. For all samples, survey spectra were acquired first with a pass energy of 90 eV, and high-resolution spectra for C 1s, O 1s, N 1s, and Fe 3p investigated were acquired in the same sequence for all samples with a pass energy of 24 eV. XPS on PDMS stamps was performed with a flood gun for charge compensation of these insulating samples. For the emission experiments a scanning system was mounted in a vacuum chamber working at a pressure of  $\approx 5 \times 10^{-7}$  mbar. A tip with a radius of 2–5  $\mu\text{m}$  was scanned over the surfaces with a stepping motor at a constant height of 3–6  $\mu\text{m}$  above the surface. The voltage (typically, 100 V) was held constant and the current was recorded every 3  $\mu\text{m}$  with a Keithley 237 source-measure unit.

### 3. Results and Discussion

Inking a PDMS stamp with catalyst precursors for  $\mu\text{CP}$  is a challenge. First, the useful solvents are restricted to water and ethanol (and perhaps methanol); higher molecular organic solvents often interfere with the chemical and topological integrity of the stamp, which leads to a swelling of the PDMS surface and ultimately to the breakdown of the homogeneous conformal contact between substrate and stamp. Second, the catalyst precursor should be soluble in sufficient concentrations in the solvent and stable for more than a few hours. Third, there must be an affinity of the catalyst to the stamp surface. We saw above that hydrophilization of the PDMS surface using an  $\text{O}_2$  plasma<sup>27,28</sup> is a prerequisite for printing catalysts.<sup>16,25</sup> All our attempts to print catalysts with hydrophobic PDMS stamps failed. Fourth, the stamp must be loaded with

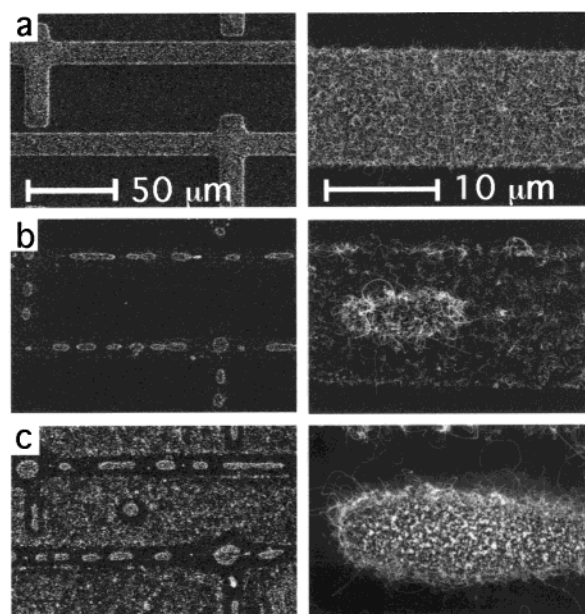


**Figure 2.** Scanning electron microscope images of a surface patterned with carbon nanotubes for three different ethanolic inks (all 40 mM inks were aged for at least 12 h): (a)  $\text{Fe}(\text{NO}_3)_3 \cdot 9\text{H}_2\text{O}$ , (b)  $\text{FeCl}_3 \cdot 6\text{H}_2\text{O}$ , and (c)  $\text{FeCl}_3$ . The images show that the catalyst precursor has to be chosen carefully and that only catalyst (a) leads to a homogeneous pattern of carbon nanotubes. The same magnification was chosen for all images in the left and right columns.

**Table 1. Influence of Various Catalysts (40 mM Aged for at Least 12 h before Use) and Solvents on the Morphology of the Patterns**

	solvent	color of ink	morphology of the pattern of nanotubes
$\text{Fe}(\text{NO}_3)_3 \cdot 9\text{H}_2\text{O}$	$\text{H}_2\text{O}$	yellow	islands
	EtOH	dark reddish brown	homogeneous pattern
$\text{FeCl}_3 \cdot 6\text{H}_2\text{O}$	$\text{H}_2\text{O}$	yellow	islands
	EtOH	yellow	islands
$\text{FeCl}_3$	$\text{H}_2\text{O}$	yellow	islands
	EtOH	yellow	islands and diffuse background

catalyst homogeneously over the complete surface. For this reason the removal of excess ink (by drying the stamp under a stream of  $\text{N}_2$  or by spin-coating) after impregnation with catalyst should not leave drying traces or cause the catalyst to crystallize. Finally, the transfer of the catalyst precursor to the substrate must be sufficient.

To evaluate the best catalytic ink, we performed a series of experiments with different transition metal salts. Table 1 reveals the catalysts printed on  $\text{SiO}_2/\text{Si}$  wafers followed by a standard deposition in acetylene. As illustrated in Figure 2, the assembly of these catalysts gives rise to three phenomena: (a)  $\text{Fe}(\text{NO}_3)_3 \cdot 9\text{H}_2\text{O}$  dissolved in ethanol is the only catalyst that results in a homogeneous film of carbon nanotubes, Figure 2a. (b) Using all other metal salts dissolved in water or ethanol (except ethanolic  $\text{FeCl}_3$ ) gives rise to patterns consisting of islands with a high density of carbon nanotubes surrounded by a film of lower density (Figure 2b). In this case, however, the carbon nanotubes are strictly confined to the lines and absent from the adjacent regions. (c) SEM images of samples activated with ethanolic  $\text{FeCl}_3$  (nonhydrated) show substrates completely covered with a diffuse background, which consists of small particles of amorphous carbon and some carbon nanotubes (Figure 2c). Using these results, we now discuss the processes involved during inking, drying, and printing.

(27) Chaudhury, M. K.; Whitesides, G. M. *Langmuir* **1991**, *7*, 1013.

(28) Chaudhury, M. K.; Whitesides, G. M. *Science* **1992**, *255*, 1230.



**3.1. Aqueous Inks.** When water is used as a solvent, we observe a yellow solution for all catalysts, which does not change within several days. UV-vis measurements of the inks as a function of their age confirmed this behavior. The absence of a change toward a dark reddish-brown color indicates that there is no major formation of Fe(III) hydroxy polymers, which is typical for the hydrolysis of Fe(III).<sup>29,30</sup> Printing these catalysts leads to islands or droplets within the printed pattern, as can be observed by optical microscopy after printing. As we see these islands on the stamp surface after drying but before printing, we conclude that they arise from a drying effect on the stamp surface. During the final drying of the stamp the water film starts to form droplets and the catalyst precursor is left in high concentration where these droplets dry out and in lower concentration on the rest of the pattern.<sup>31</sup> This inhomogeneous pattern is then printed to the surface and leads ultimately to the phenomenon observed in Figure 2b.

**3.2. Ethanolic Inks.** To suppress island formation during drying, we performed experiments using ethanol as a solvent. Ethanol has a higher vapor pressure than water, so we expected that it should dry without leaving drying traces on the stamp. The choice of the three catalysts listed in Table 1 allowed us to investigate two different important parameters without affecting the rest of the ink: the influence of crystal water and the type of ligands of the transition metal salt.

**Influence of Crystal Water.** The difference of the carbon deposit after printing either with nonhydrated or with hexahydrated ethanolic FeCl<sub>3</sub> is substantial. Printing the hydrated chloride complex results in the formation of islands, whereas printing the nonhydrated catalyst produces in addition a diffuse background over the entire surface. Both catalyst precursor solutions are yellow in color when prepared and do not change color for several weeks. This was confirmed by UV-vis measurements, which reveal the same time-independent spectrum for both catalysts. Regarding the stability of the solutions, we assume that there is again no major hydrolysis for both chloride catalysts in the solutions. For nonhydrated FeCl<sub>3</sub> dissolved in ethanol, this is in agreement with earlier results, which proved that FeCl<sub>3</sub> is in its monomeric state.<sup>32</sup> Optical images of the printed patterns of both catalysts show the same image: the lines are decorated with islands, but regions between the lines are completely free of material. We believe that in the case of the hydrated catalyst the crystal water give rise to some hydrolysis during the drying of the stamp.<sup>31</sup> Evaporating the ethanol increases the relative amount of water in the ink and forces the formation of bigger Fe(III) hydroxy polymers, which—printed to the substrate—are too large to diffuse on the surface during the 15 min of annealing at 750 °C. For the nonhydrated catalyst the polymerization during drying is strongly suppressed and the monomers or small aggregates can diffuse on the surface and produce the observed background.

**Influence of Ligands.** Catalysts with different ligands cause completely different patterns of carbon nanotubes. Replacing the chloride ligands with nitrate ligands produces a solution that turns from reddish brown to dark reddish brown within 12 h. It is known that this change

of color is due to the hydrolysis of Fe(III).<sup>29,30</sup> In turn, the nitrate-containing ink can be printed homogeneously on the substrate and catalyzes the growth of a high-quality patterned film of multiwall carbon nanotubes.<sup>33</sup>

Increasing the amount of water in the ethanolic nitrate ink (these inks showed a dark brown precipitate after a few hours) was accompanied by the occurrence of island formation (on the stamp) after printing. In fact, the UV-vis spectrum changes only a little upon addition of water, which indicates that the island formation in this case is mainly due to a drying effect caused by the additional water and not to a dramatic change of the chemistry of the catalyst.

As Fe(NO<sub>3</sub>)<sub>3</sub>·9H<sub>2</sub>O dissolved in ethanol is the only catalyst that results in homogeneous patterns, we always used this type of ink for the following experiments.

**Influence of Aging.** The change of the color of the nitrate catalyst in ethanol to dark reddish brown occurs over a few hours. However, the time needed to obtain a stable solution as well as the final degree of hydrolysis depends strongly on the ambient temperature and humidity, which should be kept constant. Printing freshly prepared nitrate catalysts always resulted in the formation of islands after printing. We suppose that the catalytic oligomers of freshly prepared solutions are small and that an important amount of unreacted crystal water is still present in the solution. This excess water is responsible for the poor drying behavior of the ink on the stamp.

**Multiple Printing.** We observed that successful printing without reinking the stamp can be performed up to 3 or 4 times, indicating a large quantity of catalyst on the stamp. Qualitative XPS measurements of the amount of Fe(III) on the stamp before and after printing confirmed this finding and showed that only some of the catalyst is transferred to the substrate during each print. This is in contrast to other catalysts (for example Pd(II)) with which printing can be executed only once.<sup>25</sup> These results are a further indication that our Fe(III) catalyst is present in a polymerized gel-like form on the stamp.

The fact that stamps can be loaded with significant amounts of Fe(III) catalysts can be used to contact-ink patterned stamps from preinked flat stamps.<sup>34</sup> In this case a flat stamp is inked first before a second patterned stamp is brought into contact to pick up the catalyst. This inking process provides another way to control the amount of catalyst to be printed because during contact inking, less than 50% of the material is transferred from the flat stamp to the patterned one. Contact inking is therefore very suitable for printing low-density patterns of catalysts without changing the chemistry of the ink solution (the degree of hydrolysis of Fe(III) depends on the concentration of the dissolved metal salt).

**Influence of Annealing.** XPS experiments of the printed catalyst before and after the 15 min of annealing indicate several interesting facts. The nitrogen N 1s peak at 407 eV from the nitrate ligands is found before the annealing but completely disappears during heating at 750 °C. At this temperature the nitrate ligands evaporate

(29) Cornell, R. M.; Schwertmann, U. *The Iron Oxides*; VCH: Weinheim, Germany, 1996.

(30) Flynn, C. M. *Chem. Rev.* **1984**, *84*, 31.

(31) Brinker, C. J.; Scherer, G. W. *Sol-Gel Science*; Academic Press: San Diego, CA, 1990.

(32) Vertes, A.; Nagy-Czakó, I.; Burger, K. *J. Phys. Chem.* **1978**, *82*, 2, 1469.

(33) To ensure that this is a true effect from the ligands, we added water to the chloride catalyst (FeCl<sub>3</sub>·6H<sub>2</sub>O dissolved in ethanol) to obtain nine (and more) water molecules for each Fe(III) atom. Adding the water did not stimulate hydrolysis of the chloride-containing catalyst. We assume that the nitrate ligands in the ethanolic solutions allow some hydrolysis, whereas the chloride inhibits it. The reason for this is not yet clear. To the best of our knowledge, there has been no study of hydrolysis of Fe(NO<sub>3</sub>)<sub>3</sub>·9H<sub>2</sub>O in ethanol. Interpreting the UV-vis spectra is difficult and we were not able to draw any conclusions regarding the reactions occurring in the solution.

(34) Libioulle, L.; Bietsch, A.; Schmid, H.; Michel, B.; Delamar, E. *Langmuir* **1999**, *15*, 300.

fully from the catalytic material. No change of the Fe 3p peak at 710.8 eV typical for Fe(III) oxides could be observed after annealing. The appearance of a small shoulder at 530 eV in the region of the O 1s peak indicates the formation of Fe–O–Fe bonds during heating, which is due to  $\text{Fe}_2\text{O}_3$ .<sup>35,36</sup> Taking these results into account, we propose the following process: the printed catalyst consists of a gel-like material of partially hydrolyzed Fe(III) nitrate, the nitrate ligands evaporate during heating, and  $\text{Fe}_2\text{O}_3$  forms.

**Summary.** Considering all these facts (the influence of crystal water, ligands, aging, etc.) leads us to conclude that the success of using an aged ethanolic solution of  $\text{Fe}(\text{NO}_3)_3 \cdot 9\text{H}_2\text{O}$  for  $\mu\text{CP}$  is based on the following:<sup>37</sup> the nitrate ligands allow the hydrolysis of Fe(III) with the crystal water, the limited amount of crystal water stops the polymerization after a few hours, the polymers are large but still soluble in ethanol, drying of the catalyst on the stamp is improved because the gel-like catalyst<sup>30,38</sup> forms a porous but uniform film, and finally most of the crystal water has reacted during the hydrolysis and cannot induce island formation during the drying step.

### 3.3. Morphology of Multiwall Carbon Nanotubes.

The investigation of methods to pattern substrates with carbon nanotubes was motivated by the strong interest in their physical properties and possible applications (for example, as cold electron emitters).<sup>39–43</sup> So far, several groups have presented various methods for patterning substrates with catalysts. It turned out that these methods are successful in producing homogeneous patterns of different types of carbon nanotubes (single-wall, multiwall, and fibers), depending on the catalyst and the deposition parameters.<sup>8,9,14–16,44</sup> However, none of these methods were able to vary the density of the carbon nanotubes within the deposited structures in a controlled way. This is a serious drawback because the emission properties of field emitters depend strongly on their local density.

**Influence of Ink Concentration.** One of the advantages of  $\mu\text{CP}$  catalysts is that they allow the density of the carbon nanotubes in the printed pattern to be tuned. This can easily be achieved by changing the density of the catalyst in the ink solution. Figure 3 shows the influence of the catalyst concentration on the topography of the deposited film.

Increasing the concentration from 10 to 40 mM is accompanied by a similar increase of the density of the deposited nanotubes (Figure 3a–c). For low concentrations (10 mM) only a few single nanotubes were distributed randomly over the printed zones. Increasing the concen-

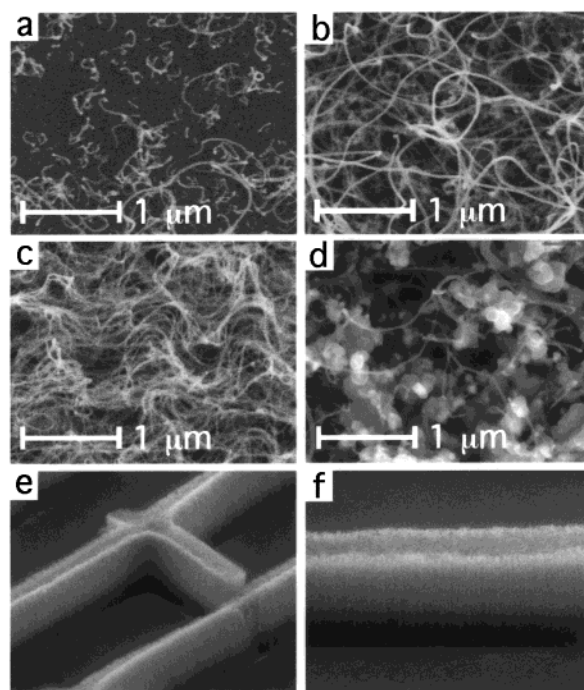


**Figure 3.** Dependence of the patterned film of carbon nanotubes on the concentration of the printed catalyst (dissolved in ethanol and aged): (a) 10 mM, (b) 25 mM, (c) 40 mM, (d) 70 mM, and (e), (f) 50 mM  $\text{Fe}(\text{NO}_3)_3 \cdot 9\text{H}_2\text{O}$ . Images (e), (f) show structures of aligned nanotubes grown perpendicular to the surface. The width of the line is 10  $\mu\text{m}$  and the height of the towers is 20  $\mu\text{m}$ .

tration of the catalyst to 20–40 mM causes a film of entangled nanotubes to form. Finally, using a concentration of around 50 mM results in arrays of nanotubes aligned perpendicular to the surface (see Figure 3e,f), similar to aligned assemblies of nanotubes found by other groups.<sup>8,10–12,44,45</sup> The side walls are flat and no tubes are branching away. High-magnification SEM images reveal that the tops of the towers are smooth without nanotubes sticking out. The transition from an entangled film obtained by using a low ink concentration to a well-aligned film of carbon nanotubes for high ink concentrations is due to a change of the nucleation density. If the nucleation density is low, nanotubes have a large volume where they can grow and a strongly entangled film is formed. The situation is different for high nucleation densities. Nanotubes grow off the nucleation centers and must extend along the direction normal to the substrate because neighboring nanotubes force them to grow in only one direction. As the tubes lengthen, they interact with their neighbors via van der Waals forces to form bundles. The attractive force is such that even the outermost nanotubes are held to the tower without branching away.

For concentrations higher than about 60 mM the growth of nanotubes is almost inhibited and the pattern is decorated by particles of carbon (Figure 3d). This result stresses the importance of the catalyst concentration: printing too much catalyst leads to the growth of a significant amount of amorphous carbon. We believe that this is due to too large a nucleation density on the substrate. In this case acetylene is decomposed at so many centers that the deposited nuclei coalesce and form large amorphous grains. We should keep in mind that there is a threshold density—given by the outer diameter of the carbon nanotubes—which determines the maximum number of tubes per surface area. If the nucleation density is higher than this threshold, a film of other carbon modifications will be formed.

(35) Armelao, L.; Bertinello, R.; Crociani, L.; Depaoli, G.; Granozzi, G.; Tondello, E.; Bettinelli, M. *J. Mater. Chem.* **1995**, *5*, 79.

(36) Al-Bawab, A.; Friberg, S. E.; Sjöblom, J.; Farrington, G. *Phys. Chem. Glasses* **1998**, *39*, 122.

(37) In addition to  $\text{Fe}(\text{NO}_3)_3 \cdot 9\text{H}_2\text{O}$  we tried using  $\text{Co}(\text{NO}_3)_2 \cdot 6\text{H}_2\text{O}$  and  $\text{Ni}(\text{NO}_3)_2 \cdot 6\text{H}_2\text{O}$  as catalysts. UV–vis measurements and observation of the color showed that no aging occurs for Co and Ni. In this sense it is not surprising that these catalysts dissolved in water and ethanol formed islands on the stamp upon drying. Beside the inorganic catalysts we tried to print organometallic catalysts (ferrocene and ferric acetylacetonate) dissolved in ethanol using either hydrophobic or hydrophilic stamps. We never succeeded in depositing carbon nanotubes on samples patterned with these catalyst precursors.

(38) Dzombak, D. A.; Morel, F. M. M. *Surface Complexation Modeling*; John Wiley & Sons: New York, 1990.

(39) De Heer, W. A.; Chätelain, A.; Ugarte, D. *Science* **1995**, *270*, 1179.

(40) Rinzler, A. G.; Hafner, J. H.; Nikolaev, P.; Lou, L.; Kim, S. G.; Tománek, D.; Nordlander, P.; Colbert, D. T.; Smalley, R. E. *Science* **1995**, *269*, 1550.

(41) Collins, P. G.; Zettl, A. *Appl. Phys. Lett.* **1996**, *69*, 1969.

(42) Che, G.; Lakshmi, B. B.; Fisher, E. R.; Martin, C. R. *Nature* **1998**, *393*, 346.

(43) Bonard, J.-M.; Salvetat, J. P.; Stöckli, T.; de Heer, W. A.; Forró, L.; Chätelain, A. *Appl. Phys. Lett.* **1998**, *73*, 918.



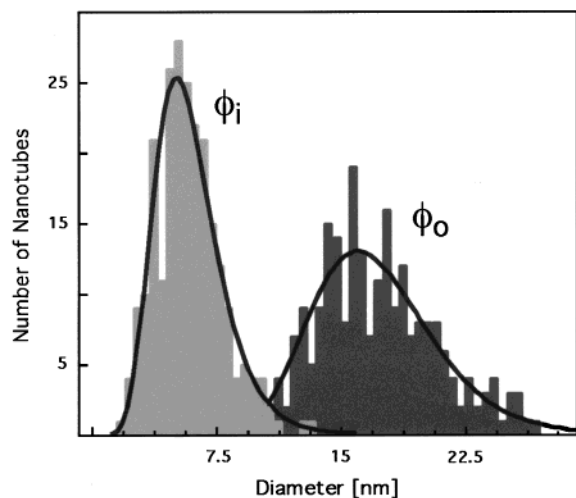


**Figure 4.** The size distributions of the inner ( $\Phi_i$ ) and outer ( $\Phi_o$ ) diameter of the multiwall carbon nanotubes show no dependence on the ink concentration nor the annealing time of the catalyst precursor. Plotted lines are log-normal fits of the data and serve as guides to the eye. Typically, the diameters of 400 tubes are evaluated for the size distributions.

To evaluate the influence of the ink concentration on the inner and outer diameter ( $\Phi_i$ ,  $\Phi_o$ ) of the multiwall carbon nanotubes, we determined the diameters for samples printed with inks of different concentrations from TEM measurements. Printing concentrations of 15, 30, and 45 mM results in tubes with an inner diameter  $\Phi_i$  of  $\approx 5.3$  nm and an outer diameter  $\Phi_o$  of  $\approx 15.4$  nm. There is no obvious trend toward larger  $\Phi_i$ 's for higher ink concentrations. The histogram in Figure 4 shows a typical size distribution of the diameters. The maxima of the  $\Phi_i$  distributions for all three ink concentrations is located within  $\pm 0.5$  nm around 5.3 nm, whereas the values of  $\Phi_o$  are spread  $\pm 3.2$  nm around 15.4 nm. We attribute the larger variation of  $\Phi_o$  to slightly different amounts of acetylene arriving at different positions in our deposition chamber and not to an effect from the catalyst.

**Quality of Multiwall Carbon Nanotubes.** Figure 5a,b show TEM images of the structure of the carbon nanotubes. They reveal the typical structure of multiwall carbon nanotubes produced by catalytic decomposition: well-graphitized walls aligned with the tubes' axis and some defects. These images show the high selectivity of the deposition process: the catalytic decomposition of acetylene gas over the catalytic pattern leads almost exclusively to the growth of carbon nanotubes.

**Influence of Annealing Time.** To examine the influence of the annealing time—which could change the size and topography of the catalyst—on the carbon nanotubes, we measured their diameters for samples printed with 40 mM ink but annealed for 0, 15, and 30 min under  $N_2$ . The results reveal that annealing at 750 °C has no influence on the diameters.  $\Phi_i$  and  $\Phi_o$  for all three annealing times exhibit size distributions, which are very similar to the one shown in Figure 4. TEM measurements of the printed ink at the border of a thin sample,<sup>46</sup> presented in Figure

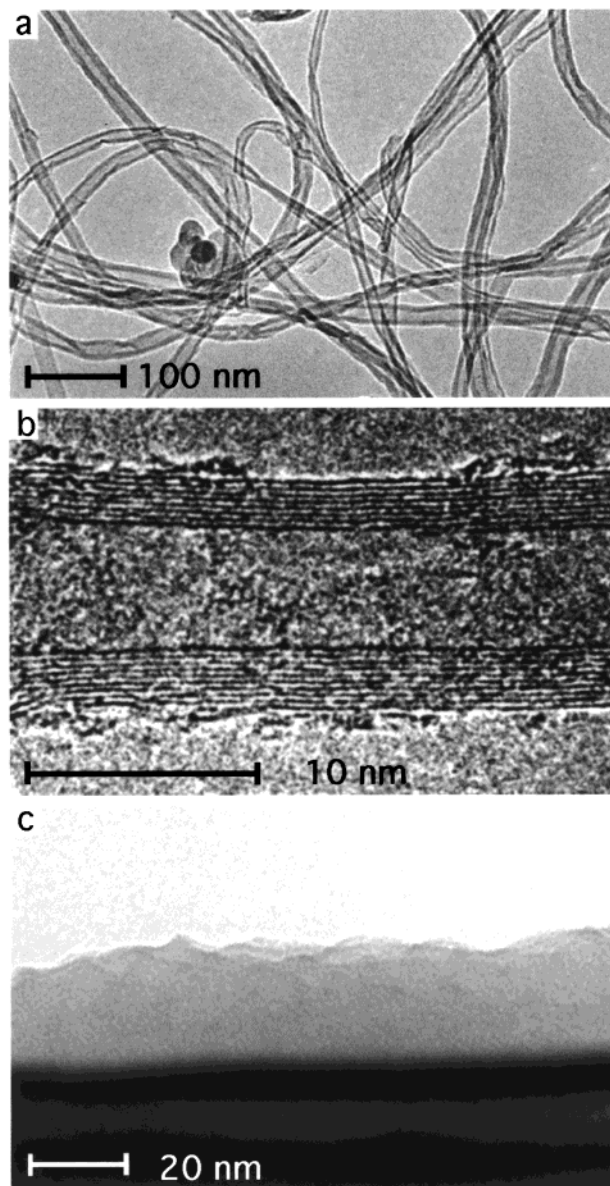


**Figure 5.** Transmission electron microscopy images showing (a) the composition (with no purification) of the deposited film of multiwall carbon nanotubes and (b) their structure. (c) TEM image of the cross section through a printed and annealed film of catalyst at the border of a thin substrate, revealing the amorphous and continuous nature of the catalyst.

5c, show that the annealed ink forms a compact amorphous film with a surface roughness of a few nanometers. Colloidal particles cannot be resolved in this material. Hence, such particles must be smaller than 1 nm or are absent. The annealing of the printed catalysts (gel-like polymer containing Fe(III) hydroxo species and ethanol) is probably fast and leads for all samples to a similar topography of the catalytic film, independent of the annealing time.

**Influence of Substrate.** The choice of an appropriate substrate is very critical. Besides printing on the native oxide of silicon wafers, we printed on quartz, HOPG, Au, and nanoporous silicon. Glass shows the same behavior as silicon and can easily be patterned with nanotubes. Printing on HOPG and Au(111) results in patterns decorated with islands of amorphous carbon. Apparently, the surface free energy of these surfaces has an important influence on the behavior of the catalyst. It is not yet clear whether the failure to achieve a homogeneous patterning

(44) Ren, Z. F.; Huang, Z. P.; Wang, D. Z.; Wen, J. G.; Xu, J. W.; Wang, J. H.; Calvet, L. E.; Chen, J.; Klemic, J. F.; Reed, M. A. *Appl. Phys. Lett.* **1999**, *75*, 1086.

(45) Li, J.; Papadopoulos, C.; Xu, J. M.; Moskovits, M. *Appl. Phys. Lett.* **1999**, *75*, 367.

(46) The printed ink was characterized by mounting a thin cleaved sample on a TEM grid with the electron beam at an angle of 45° incidence to the substrate surface. Measurements were performed at the edge of the substrate surface. The method used here is described in Bonard, J.-M.; Ganière, J.-D.; Morier-Genoud, F.; Achtenhagen, M. *Semicond. Sci. Technol.* **1996**, *11*, 410.

occurs during printing or annealing; this will require further investigation. Printing on nanoporous silicon is not successful because the effective surface in contact with the stamp during printing is much smaller than that for printing on a flat surface. In turn, very little catalyst is transferred to the substrate and ultimately only a few nanotubes can be found after deposition with acetylene.

**Influence of Deposition Parameters.** To obtain a rough estimate of the importance of the various deposition parameters on the morphology of the carbon nanotubes, a series of different depositions were carried out: a strong influence of temperature was not visible by SEM in the region between 650 and 800 °C. The multiwall carbon nanotubes always show a similar morphology. Decreasing the deposition temperature to 620 °C inhibits the growth of the nanotubes. Apparently, the minimum temperature for the production of nanotubes is around 630 °C for our deposition system. Increasing the temperature to more than 800 °C is accompanied by an increased deposition of particles of amorphous carbon within the film and on the walls of the nanotubes. Using Ar or a 10/90 vol % mixture of NH<sub>3</sub> and N<sub>2</sub> as the carrier gas changes the morphology of the carbon nanotubes: the deposited films are more entangled, the length of uncurved regions of the nanotubes decreases, and a larger amount of amorphous particles is found. Reduction of the catalyst in a hydrogen gas before deposition leads to a similar appearance. All these different gas treatments result in tubes of smaller dimensions ( $\Phi_1 \approx 3.2$  nm and  $\Phi_0 \approx 11.6$  nm) compared to the tubes produced in a standard deposition with pure N<sub>2</sub>. We think that this is due to a different behavior of the printed ink during annealing in the various gases. Nevertheless, the best quality of the carbon nanotubes is always obtained when N<sub>2</sub> is used as the carrier gas without adding NH<sub>3</sub> or prereducing the catalyst in hydrogen. We have not examined in detail the influence of the other gases for this reason. Taking these results into account, we emphasize that the deposition parameters appear to have a weaker impact on the final film than does the composition of the ink.

**3.4. Electron Emission Properties of Patterned Substrates.** Substrates patterned with carbon nanotubes have been proposed as cold electron sources for flat-panel devices.<sup>39,40,47</sup> Nanotubes exhibit a very high length-to-diameter ratio, are chemically and physically inert, support high electric currents, are patternable, and can be produced by simple and inexpensive methods. Measuring the local field emission of electrons should reproduce the deposited pattern of nanotubes and provide a good test of the selectivity of the emission process: electrons should only be emitted from areas covered with nanotubes.

A scanning anode field emission microscope was used to measure the local emission properties of the samples: a tip with a radius of  $\approx 3 \mu\text{m}$  was scanned over the sample at constant height with a constant applied voltage of typically 100 V. The resulting field emission current (up to 10  $\mu\text{A}/\text{pixel}$ ) was acquired every 3  $\mu\text{m}$ .<sup>48</sup> Figure 6 shows the emission image of a sample printed with a 20 mM concentration, which corresponds to a density of carbon nanotubes similar to the one shown in Figure 3b. The image reproduces nicely the lines of the printed pattern, and emission of adjacent regions is strongly suppressed. Line widths are broadened ( $\approx 15 \mu\text{m}$ ) because the emission image is a convolution of tip apex, tip-sample distance, and the height of the deposited nanotubes. In the upper

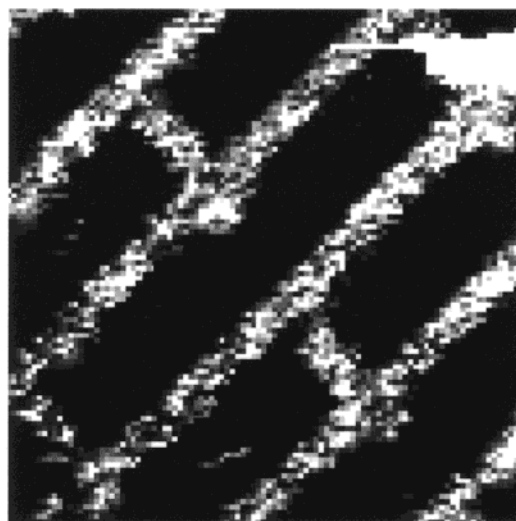


**Figure 6.** Emission image of a patterned substrate recorded with a tip scanned over the surface at a height of 5  $\mu\text{m}$  and an applied voltage of 100 V. The intensity scale varies from no current for black pixels to a maximum of 10  $\mu\text{A}/\text{pixel}$  for bright pixels.

right corner a bright spot appeared because one or more nanotubes branched out of the film and touched the tip during scanning. Samples consisting of a higher or lower density of carbon nanotubes reproduce the pattern but exhibit a decreased density of emitting centers. This highlights the importance of controlling the density of the carbon nanotubes within the patterned features. More details on the emission properties of patterns of different densities of carbon nanotubes are reported elsewhere.<sup>48</sup>

#### 4. Conclusion

What is the advantage of using  $\mu\text{CP}$  of catalysts to pattern substrates with carbon nanotubes by the catalytic decomposition of hydrocarbons? Our results suggest that printing a gel-like polymerized catalyst is an enticing alternative to the usual lithographic techniques: the growth process leads to a carbon deposit consisting of almost 100% multiwall carbon nanotubes, the contrast achieved is excellent, and the density of nanotubes within the pattern can be tuned. PDMS, the elastomeric material used in soft lithography, is fully compatible with many other wet catalysts, is cheap, and can be scaled up. The choice of wet catalysts opens the possibility of investigating a new class of customer-designed catalysts, which allow better control over the inner and outer diameter of the nanotubes, the density of the nanotubes in the film, and their orientation on the substrate.

**Acknowledgment.** We thank E. Delamarche, M. Geissler, B. Michel, and H. Schmid for providing us with masters and stamps and A. Bietsch and A. M. Bittner for helpful discussions. We are grateful to CIME-EPFL for access to SEM and TEM facilities. K. Hernadi gratefully acknowledges the financial support of the National Science Foundation of Hungary (OTKA T025246). We thank N. Xanthopoulos of the Surface Analysis Laboratory at EPFL for performing the XPS measurements and P. Bugnon (IGA-EPFL) for his help with the gas reactor.

(47) Bonard, J.-M.; Salvetat, J.-P.; Stöckli, T.; Forró, L.; Châtelain, A. *Appl. Phys. A* **1999**, *69*, 245.

(48) Nilsson, L.-O.; Gröning, O.; Emmenegger, C.; Küttel, O.; Maillard-Schaller, E.; Schlapbach, L.; Kind, H.; Bonard, J.-M.; Kern, K. *Appl. Phys. Lett.* **2000**, *76*, 2071.